

Human non-rapid eye movement stage II sleep spindles are blocked upon spontaneous K-complex coincidence and resume as higher frequency spindles afterwards

VASILEIOS KOKKINOS and GEORGE K. KOSTOPOULOS

Neurophysiology Unit, Department of Physiology, Medical School, University of Patras, Rion, Greece

Accepted in revised form 24 December 2009; received 05 August 2009

SUMMARY The purpose of this study was to investigate a potential relation between the K-complex (KC) and sleep spindles of non-rapid eye movement (NREM) stage II of human sleep. Using 58 electroencephalogram electrodes, plus standard electrooculogram and electromyogram derivations for sleep staging, brain activity during undisturbed whole-night sleep was recorded in six young adults (one of them participated twice). NREM stage II spindles (1256 fast and 345 slow) and 1131 singular generalized KCs were selected from all sleep cycles. The negative peak of the KC, the positive peak of the KC (where applicable), and the prominent negative wave peak of slow and fast spindles were marked as events of reference. Fast Fourier transform-based time–frequency analysis was performed over the marked events, which showed that: (a) fast spindles that happen to coincide with KC are interrupted (100% of 403 cases) and in their place a slower rhythmic oscillation often (80%) appears; and (b) spindles that are usually (72% of 1131) following KCs always have a higher frequency (by ~1 Hz) than both the interrupted spindles and the individual fast spindles that are not in any way associated with a KC. This enhancement of spindle frequency could not be correlated to any of the KC parameters studied. The results of this study reveal a consistent interaction between the KC and the sleep spindle during NREM stage II in human sleep.

KEYWORDS human electroencephalogram, k-complex, non-rapid eye movement sleep, spindle

INTRODUCTION

The second stage of the human non-rapid eye movement (NREM) sleep is characterized by two major electroencephalogram (EEG) graphoelements: the K-complex (KC) and the sleep spindle. The KC is a delineated biphasic slow wave, starting with a negative phase that may or may not be immediately followed by a positive phase (Amzica and Steriade, 2002; Colrain, 2005; Halász, 2005). The sleep spindle is a clearly distinguishable oscillatory rhythm of a waxing and waning shape (De Gennaro and Ferrara, 2003). Two types of sleep spindles have been described: fast spindles of a centro-

parietal dominance and a frequency varying ~ 14 Hz; and slow spindles of a frontal distribution and a frequency varying ~12 Hz (Gibbs and Gibbs, 1964).

Although the KC was first described by Loomis *et al.* (1938) 70 years ago, its functional role is still a debatable issue. The KC can appear either spontaneously or can be elicited by external stimuli, is accompanied by autonomic alterations (Hornyak *et al.*, 1991; Okada *et al.*, 1991; Roth *et al.*, 1956; Takehuchi *et al.*, 1994; Tank *et al.*, 2003), and may be followed by arousals; therefore, it is considered by some to be an arousal reaction. Other investigators argue that it is a sleep-protecting mechanism, inhibiting arousals and promoting cortical processing (Colrain, 2005). Similarly, since its first description by Loomis *et al.* (1936), the function of the sleep spindle also remains undefined. There are data supporting its role as an arousal inhibitor and thus a sleep preservation

Correspondence: George Kostopoulos, Neurophysiology Unit, Department of Physiology, University of Patras, 26500, Rion, Greece. Tel.: +302610-969157; fax: +302610-997215; e-mail: gkkostop@med.upatras.gr

mechanism (Yamadori, 1971). There are also data supporting a role of spindles in memory consolidation during sleep (Gais *et al.*, 2002).

The idea of an antagonistic scheme between the KC and the sleep spindle has progressively developed in literature. Ehrhart *et al.* (1981) investigated the occurrence of both EEG phenomena before transient arousals during sleep, and found that there is a lower incidence of sleep spindles in the 10-s interval before the microarousal and an increase in KC appearance. Benzodiazepine administration has been shown to increase spindle appearance and decrease KCs (Gaillard and Tissot, 1975; Johnson *et al.*, 1976; Kubicki *et al.*, 1987; Naitoh *et al.*, 1982). Halász (1993) reported a suppression of spindles for 5–15 s following evoked KCs, and so proposed that KCs are Janus-face responses to arousal inputs, as they combine a slow wave maintaining the continuity of sleep with an ability of non-oscillating thalamocortical (TC) circuits to import information. The role attributed to the KC as being the forerunner of delta waves of slow-wave sleep (SWS) supported an inverse relation between KCs and sleep spindles, in accordance with the inverse relationship between delta waves and sleep spindles (De Gennaro and Ferrara, 2003; De Gennaro *et al.*, 2000). On the contrary, there are data supporting independent roles for both KCs and sleep spindles. Church *et al.* (1978) showed that the application of auditory stimuli during either the presence or the absence of a sleep spindle did not inhibit the occurrence of KCs but, moreover, evoked higher KCs. In addition, auditory stimuli during spindle bursts produced no significant cardiovascular responses. The KC versus spindle interaction results of Church *et al.* (1978) were confirmed by Crowley *et al.* (2004), and further complemented by the absence of age-related effects. Spindle occurrence is increased while spontaneous KCs are reduced throughout the night (Curcio *et al.*, 2003). Finally, in terms of pacing mechanisms, spindles are thought to be paced by TC circuits, whereas KCs by intracortical networks, rather independently of the thalamus (Amzica and Steriade, 2002).

The main objective of this study was to investigate a potential relation between the KC and the sleep spindle, an idea derived from the fact that they characterize the same stage of sleep. More specifically, the question set was: 'If the two phenomena are somehow related, then upon their coincidence shouldn't one of them influence one or more characteristics of the other?'. This study differs from past approaches that investigated the relation between KC and spindles in the application of event-related techniques on manually selected and sorted EEG epochs according to prominent features of those two EEG elements. We distinguished and selected singular generalized spontaneous KCs, that is, KCs not immediately preceded or followed by another KC or slow-wave activity, distinguishable across the midline electrodes, occurring spontaneously. We also distinguished and selected both slow and fast spindles in order to determine which group interacts with the KC. The event-related methodology was powered by time-frequency analysis and electrode space mapping.

MATERIALS AND METHODS

Subjects and procedures

Six individuals (one male and five females) aged between 27 and 33 years (mean age 28.8 ± 2.56 years) volunteered to participate in this study. One of the subjects participated twice, to check for reproducibility of sleep features, thus completing a total of seven nocturnal sleep recordings. All participants were good sleepers, without any difficulties in falling or remaining asleep during the night. They were all in good health and free from medication at the time of study. None of the subjects reported a history of neurological or psychiatric disorder, or disordered sleep. Subjects kept a 7-day sleep diary, and were instructed to follow their regular sleep schedule, and refrain from alcohol and caffeine at least 3 and 1 days, respectively, prior to the experiment. Menstrual phase was not controlled for in female subjects. All participants read and signed an informed consent form, which described in detail the procedures and purposes of the study.

Subjects were instructed to arrive at the laboratory ~ 1 h prior to their usual bedtime, the latter calculated as a 7-day bedtime average based on their sleep diaries. Each of them spent one whole night in the laboratory, in an air-conditioned soundproof temperature controlled dark Faraday-cage room that was intentionally not monitored to avoid potential sleep disturbances owing to the feeling of 'being watched'. No pharmacological substance was used to induce sleep. Before sleep, 2 min of recording was taking place, during which the subjects were instructed to keep their eyes closed and relax. Night sleep recording began after the subjects willingly switched off the room lights, as were instructed to do when they would feel like falling asleep, and ended with their spontaneous wake up in the morning. Electrophysiological signals were monitored in an adjacent room and overnight communication with the subjects was established vocally through a microphone-speaker console system. In the morning, all subjects reported to have had a comfortable and undisturbed sleep.

Recording

All-night sleep was recorded using 58 EEG tin electrodes according to the extended international 10–20 system (FP₁, FP₂, FP₃, F₃A, F₄A, F₇, F₅, F₃, F₁, F₂, F₄, F₆, F₈, C₅A, C₃A, C₁A, C₂A, C₄A, C₆A, T₃, C₅, C₃, C₁, C₂, C₄, C₆, T₄, T₃L, TCP₁, C₃P, C₁P, P₂A, C₂P, C₄P, TCP₂, T₄L, T₅, P₅, P₃, P₁, P₂, P₄, P₆, T₆, CB₁, P₃P, P₁P, P₂P, P₄P, CB₂, O₁, O₂, O₂) using an electrode cap (ElectroCap International, Eaton, OH, USA), that provided inter-electrode spacing of ~ 4.5 cm. EEG electrode inputs were ear lobe referenced and grounded over the F₂A position. A bipolar derivation of oblique electrooculogram was used to detect eye movements, for which electrodes were placed 1 cm above the right outer cantus and 1 cm below the left outer cantus, and a bipolar EMG from the upper masseter muscle was used to track muscle tone changes. Impedance of all electrodes was kept below 10 kOhms for most of the night. All electrophysiological

parameters were AC recorded, amplified at a total gain of 1000, band-pass filtered at 0.05–500 Hz and digitized through an 16-bit resolution A/D converter, which provided an accuracy of 0.084 $\mu\text{V}/\text{LSB}$, at a sampling frequency of 2500 Hz by a Synamps system (Neuroscan, Charlotte, NC, USA), and stored on hard disk. The 50-Hz notch filter was not applied during recording. Subject movements during sleep were detected by a sensitive motion detector placed over the bed area that produced a 2-s Transistor-Transistor Logic signal every time movement occurred. The motion detector's signal was recorded as an external trigger and was stored along with the electrophysiological signals as an event channel.

Scoring and event selection

Sleep staging was performed by visual inspection according to the standard criteria of Rechtschaffen and Kales (1968). Scoring was further aided by the collation of a Fast Fourier Transform (FFT)-based hypnospectrogram, that is, the whole-night FFT-based time–frequency plot for 0.05–45 Hz with a step frequency of 0.05 Hz. Continuous scoring was performed rather than epoch-based scoring to obtain a precise match between the derived hypnogram and the hypnospectrogram (Fig. 1). This was achieved by examining a 20-s EEG epoch and marking on it any intra-epoch changes (stage transitions or brief microarousals) with ~ 1 s. Microarousals were scored according to the guidelines of the ASDA Report (1992). Note that the hypnogram was formed with a step of only 1 s. The cumulative duration of microarousals was within normal limits (Table 1), and much shorter than the graphics compression of the hypnogram in Fig. 1 may imply.

In Table 2, we present the incidence and average peak frequency values of the basic rhythms that were observed in this study for every subject.

The KC was identified – based on standardized criteria of the AASM Visual Scoring Task Force (2007) as well as those

of the DGSM Task Force (2006) – as a > 500 -ms well-delineated negative sharp wave usually followed by a positive phase that stands out of the EEG background (Fig. 2a,b). In this study, singular (without another KC or slow-wave activity immediately preceding or following) generalized (distinguishable in the EEG all across the midline electrodes) spontaneously occurring KCs from only NREM stage II periods of the whole-night sleep of our subjects were selected. For the needs of this particular study, KCs were further categorized as $\text{KC}_{X_{-}X_0X_{+}}$, where $X_{-} \in \{0,1\}$ and denotes the absence (0) or existence (1) of a spindle interrupted by the KC, $X_0 \in \{0,1\}$ and denotes the absence (0) or existence (1) of an oscillation during the negative phase of the KC, and $X_{+} \in \{0,1\}$ and denotes the absence (0) or existence (1) of a spindle starting during the descending negative and the positive phase of the KC (see raw data images of Table 3). KCs immediately preceding microarousals and awakenings during sleep, as well as KCs followed by alpha or delta waves, were excluded from this study.

The sleep spindle was identified as a > 500 -ms train of ~ 11 – 16 -Hz waves. In this study, two types of sleep spindles were further identified as slow and fast spindles according to the definitions of Gibbs and Gibbs (1964). Fast spindles (> 13 Hz) exhibit a symmetric bilateral distribution over centro-parietal areas, while slow spindles (< 13 Hz) exhibit a similarly bilateral distribution frontally and are absent or significantly diminished in the centro-parietal and posterior areas (Figs 3 and 4). All spindles, both slow and fast, were selected from only NREM stage II periods of the whole-night sleep of our subjects. Posterior alpha rhythm was derived from the eyes-closed relaxed awareness presleep recording.

Analysis

Manual cursor marking offered by Scan software (Neuroscan, Charlotte, NC, USA) was used to create event channels.

Figure 1. The FFT-based whole-night time–frequency plot of EEG power (hypnospectrogram) derived from the Cz electrode (upper) and the respective hypnogram (lower) (MA, microarousal; AW, awake; REM, rapid-eye movement sleep; SI–IV, NREM sleep stages I–IV) of subject 1. The horizontal lines appearing at high frequencies are 50-Hz noise byproducts.

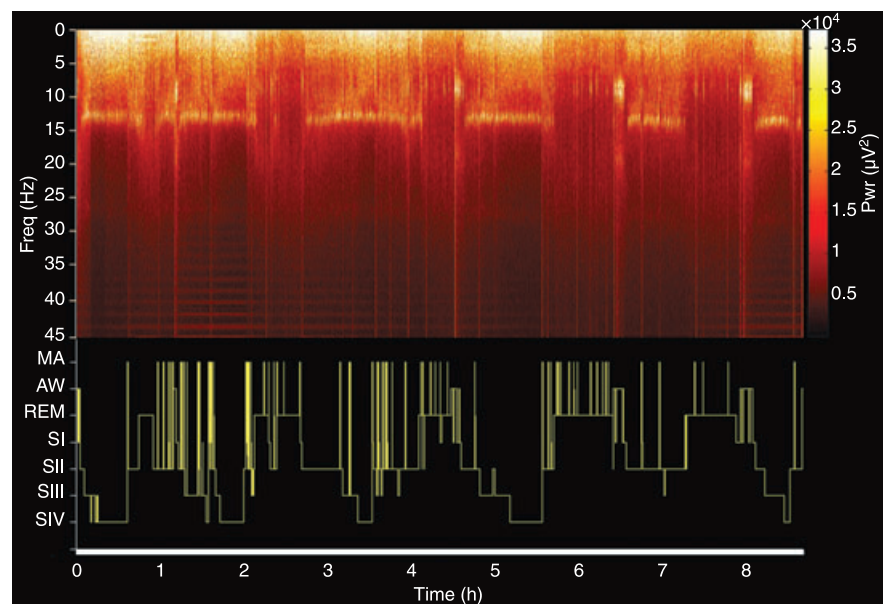


Table 1 Sleep parameters

Variables	Values
Total sleep time (min)	412.07 ± 81.81
Wakefulness after sleep onset (min)	20.52 ± 16.67
% Wakefulness after sleep onset	5.12 ± 5.03
Sleep efficiency index	93.60 ± 4.95
Sleep stage (min)	
Stage I	27.13 ± 15.47
Stage II	118.40 ± 45.91
Stage III	99.61 ± 42.25
Stage IV	58.57 ± 17.29
Rapid eye movement sleep	63.79 ± 30.41
Microarousals	25.53 ± 12.34
Sleep stage (% of total sleep time)	
Stage I	6.50 ± 3.10
Stage II	28.07 ± 8.10
Stage III	24.71 ± 9.67
Stage IV	18.96 ± 11.11
Rapid eye movement sleep	15.12 ± 5.18
Microarousals	6.20 ± 2.58
Values are mean ± SD.	

NREM stage II epochs from the whole-night sleep recording and free of any movement and other artifacts were selected, and precise time-markers were placed over the events under study. In total, four kinds of events were visually marked and used for further analysis: (a) the peak of the negative phase of the KC; (b) the peak of the positive phase of the KC (where applicable); (c) the peak of the maximum in amplitude negative

wave of the fast spindle; and (d) the peak of the maximum in amplitude negative wave of the slow spindle. For all markers, the peak was marked over the record of the Cz electrode, where fast spindles are prominent, except for the slow spindles' marker that was positioned over the record of the Fz electrode where slow spindles stand out.

Event-related data were further processed by a custom-made Matlab-based (The Mathworks, Natic, MA, USA) software suite developed at the Neurophysiology Unit. FFT-based event-related time–frequency analysis was performed for each selected event within a time-window centered (time = 0.00) at the marked event, from 0.05 to 20 Hz at a step of 0.05 Hz. In particular, slow as well as fast spindles were analyzed in a time-window of –1.00 to 1.00 s, the negative peak of the KC was coarsely analyzed in a time-window of –2.00 to 2.00 s, and the positive peak of the KC was analyzed in a time-window of –0.50 to 0.50 s. Coarse analysis resulted in averaging of the time–frequency plots (Fig. 2d) for all samples for each category of events. Moreover, the EEG related to the negative peak of the KC (time = 0.00) was finely FFT-based time–frequency analyzed in three equal and symmetrical time-windows, the first covering the time interval of –1.50 to 0.00 s, the second –0.75 to 0.75 s, and the third 0.00–1.50 s. The fine analysis was performed for each of the marked samples in order to obtain, from each of the three time intervals, the peak frequency value, and the power spectral density (PSD) of the KC-interrupted spindle, the oscillation within the KC, and the post-KC spindle, respectively, where applicable depending on the KC $KC_{X-X_0X_+}$ type. PSD values appear as the dB

Table 2 Average peak frequency values of the basic rhythms that were observed in this study for every subject (subject 4 slept twice), from a total of 1131 KCs and 1601 spindles (345 slow and 1256 fast)

	<i>Subject 1</i>		<i>Subject 2</i>		<i>Subject 3</i>		<i>Subject 4 (first night)</i>	
	<i>Peak frequency (Hz)</i>	<i>Samples</i>	<i>Peak frequency (Hz)</i>	<i>Samples</i>	<i>Peak frequency (Hz)</i>	<i>Samples</i>	<i>Peak frequency (Hz)</i>	<i>Samples</i>
Posterior alpha	9.15 ± 0.83	2 min	10.22 ± 0.85	2 min	11.14 ± 0.33	2 min	10.68 ± 0.68	2 min
Slow spindles	12.00 ± 0.55	93	12.90 ± 0.68	72	12.10 ± 0.55	13	11.80 ± 0.70	40
Fast spindles	13.60 ± 0.51	235	14.60 ± 0.76	240	13.95 ± 0.81	111	15.10 ± 0.83	196
Pre-KC spindles	13.47 ± 0.65	60/207	14.78 ± 0.55	105/233	14.13 ± 0.76	22/62	14.47 ± 1.16	67/195
KC oscillation	8.34 ± 1.38	186/207	8.07 ± 1.23	152/233	8.13 ± 1.24	51/62	9.37 ± 1.17	152/195
Post-KC spindles	14.49 ± 0.69	175/207	15.67 ± 0.77	165/233	14.81 ± 0.75	37/62	15.93 ± 0.75	128/195
	<i>Subject 5</i>		<i>Subject 6</i>		<i>Subject 4 (second night)</i>		<i>Across-subject means</i>	
	<i>Peak frequency (Hz)</i>	<i>Samples</i>	<i>Peak frequency (Hz)</i>	<i>Samples</i>	<i>Peak frequency (Hz)</i>	<i>Samples</i>	<i>Peak frequency (Hz)</i>	<i>Samples</i>
Posterior alpha	9.92 ± 0.57	2 min	11.44 ± 0.42	2 min	10.59 ± 0.73	2 min	10.44 ± 0.63	14 min
Slow spindles	11.15 ± 0.45	37	12.85 ± 0.68	47	11.40 ± 1.07	43	12.02 ± 0.66	345
Fast spindles	12.65 ± 0.72	232	14.25 ± 0.53	160	14.90 ± 0.44	82	14.15 ± 0.65	1256
Pre-KC spindles	12.56 ± 0.84	52/115	14.26 ± 0.43	46/139	14.82 ± 0.61	51/180	14.11 ± 0.71	403/1131
KC oscillation	8.81 ± 1.34	99/115	9.29 ± 1.03	106/139	9.79 ± 1.01	128/180	8.82 ± 1.20	874/1131
Post-KC spindles	13.34 ± 0.84	69/115	14.98 ± 0.52	104/139	15.75 ± 0.56	137/180	14.99 ± 0.69	815/1131

For each subject we selected all KCs fulfilling the named criteria (i.e. 207 for subject 1). Pre-KC spindles, KC oscillation and post-KC spindles were all KC_{1XX} , KC_{X1X} , and KC_{XX1} , respectively (i.e. 60, 186, and 175). All values were measured over the Cz electrode, except for the slow spindles values that were measured over the Fz electrode and the posterior alpha values that were measured over the Oz electrode. Values are means ± SD, unless otherwise indicated.

KC, K-complex.

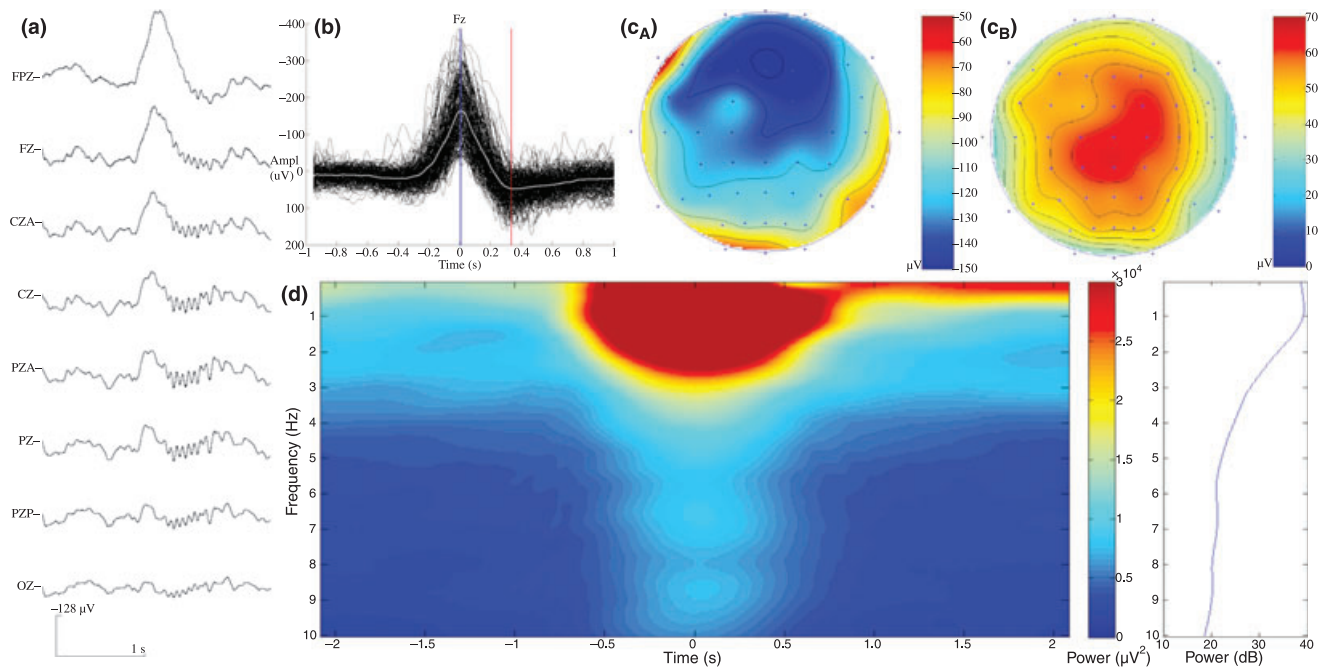


Figure 2. The KC: raw EEG of a NREM stage II KC (a), waveform superposition and average (white) of 195 KCs from subject 4's first night of sleep (b), the topographical sketches of the averaged negative (c_A) and positive (c_B) peaks of the KC, and the averaged time–frequency plot of the KCs' power derived from the Fz electrode along with the respective PSD graph (vertical curve on the right, d). The blue and red vertical lines in (b) mark the negative and positive peaks of KC, respectively.

magnitude of the spectral analysis, that is, as $10 \times \log_{10} [\text{power}_{\mu V^2}]$ over the selected time interval. The peak frequency of occipital alpha rhythm during relaxed awareness was calculated by epoching and FFT of the 2–3-min presleep recording. Scalp mapping of the recorded data was performed by the use of the Green-function-based multiquadric interpolation method described by Sandwell (1987), after baseline correction of all channels. No filter was applied to the processed electrophysiological data. All frequency and PSD values were measured over the Cz electrode, unless otherwise stated.

RESULTS

KCs

A total of 1131 KCs were accumulated from NREM stage II periods in seven whole-night EEG recordings of six subjects (one subject slept twice to control for the constancy of sleep architecture and brain rhythm characteristics) using the criteria described in section 'Materials and methods'. The time and space distribution as well as the frequency content of the studied KCs were similar to the ones already described in literature (Colrain, 2005; De Gennaro *et al.*, 2000; Halász, 200), that is, a more than 500-ms wave of significant amplitude (~ 50 –400 uV) with a prevalence of the negative peak over the frontal areas (Fig. 2a–c). The positive peak of the KC samples exhibited a dominant distribution over the central and anterior parietal areas (Fig. 2b,c).

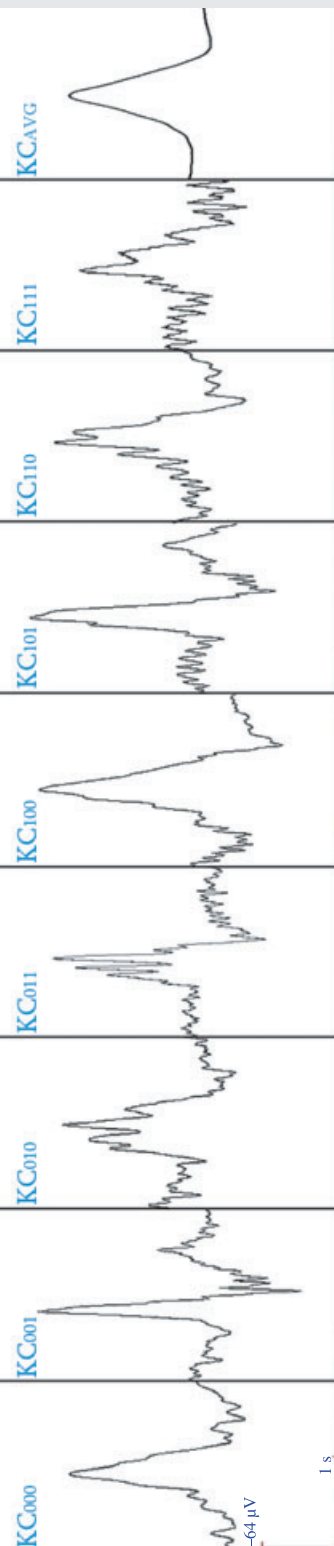






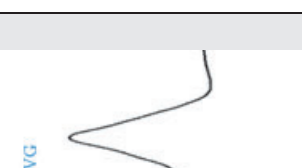
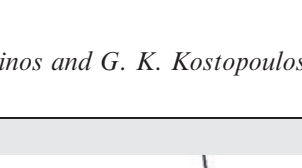
Sleep spindles

Individual spindles, that is, spindles not coinciding with KCs or other prominent EEG features, in total 1601 (345 slow spindles and 1256 fast spindles), were studied throughout all NREM stage II epochs of the seven whole-night sleep recordings. In confirmation of the previously described distinction (De Gennaro and Ferrara, 2003; Schabus *et al.*, 2007; Urakami, 2008), sleep spindles extracted from the sleep recordings of this study were either slow (of mean frequency 12.02 ± 0.66 Hz and maximal distribution over the frontal and prefrontal electrodes) or fast (of mean frequency 14.15 ± 0.84 Hz and maximal distribution over the central and anterior-parietal electrodes), as can be seen in Figs 3 and 4. Notably, both slow and fast sleep spindles compared with the EEG background were accompanied by a decrease in EEG power at frequencies 2–4 Hz (see averaged spectral graphs of Fig. 4).

Post-KC spindles are higher frequency spindles

Sleep spindles appeared right after the negative peak of KC (reaching maximum within 1 s from the negative peak of the KC, that is, during the late part of the negative and/or during its positive phase) in 814/1131 (71.97%) of the times KCs were observed. Although not precisely time-locked to the KC, we will call these spindles 'post-KC spindles' to distinguish them from 'sporadic spindles' appearing at random times, without being preceded or followed by KCs. Post-KC spindles had the

Table 3 Classification of KC types

	KC ₀₀₀	KC ₀₀₁	KC ₀₁₀	KC ₀₁₁	KC ₁₀₀	KC ₁₀₁	KC ₁₁₀	KC ₁₁₁	KC _{AVG}
									
Pre-KC (Hz)	–	–	–	–	14.37 ± 0.87	13.80 ± 0.80	14.17 ± 0.82	14.00 ± 0.83	14.08 ± 0.24
Intra-KC (Hz)	–	–	8.91 ± 0.72	8.81 ± 0.59	–	–	8.80 ± 0.85	8.89 ± 0.83	8.85 ± 0.05
Post-KC (Hz)	–	15.00 ± 0.87	–	14.92 ± 0.96	–	15.08 ± 0.92	–	15.15 ± 0.91	15.03 ± 0.09
Samples	35 (3.09%)	141 (12.46%)	116 (10.25%)	436 (38.54%)	36 (3.18%)	45 (3.97%)	129 (11.40%)	193 (16.90%)	1131

Exemplary EEG traces (top), average TFAs (middle) and frequency statistics (bottom). [The peak frequencies of the rhythms that concern this study, that is, pre-KC, the oscillation during the negative phase of the KC (intra-KC) and the post-KC spindles appear clustered according to the type of KC. The last column shows the mean frequency values across subjects. The raw data images show the KC_{X₀X₁} categorization: X_– stands for the absence (0) or existence (1) of a spindle interrupted by the KC, X₀ stands for the absence (0) or existence (1) of an oscillation during the negative phase of the KC, and X₊ stands for the absence (0) or existence (1) of a spindle triggered during the descending negative and positive phase of the KC. The spectral images [for frequencies 0.05 Hz (top) to 20 Hz (bottom), for a time interval of ± 2 s from the negative peak of the KC] are taken from 179 KCs of the second night of Subject 4's sleep. In the last column, the raw data and spectral images are both averages from the same subject. Values are means ± SD, unless otherwise indicated.

KC, K-complex.

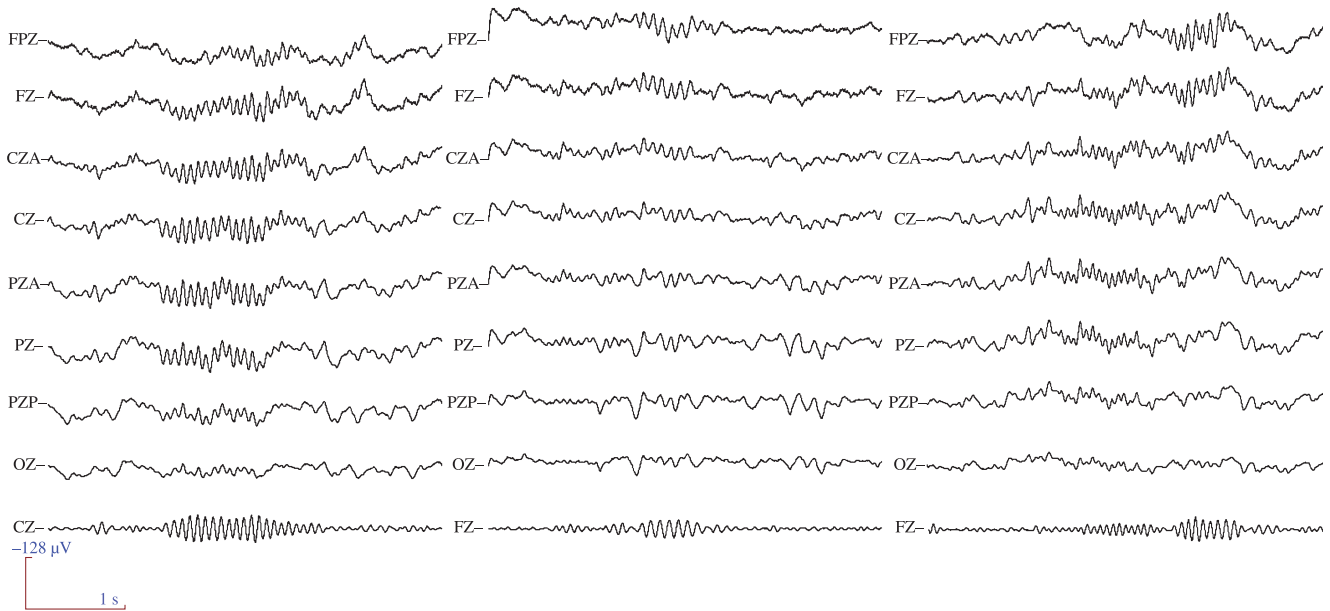


Figure 3. The sleep spindles: raw EEG of a fast spindle (left), a slow spindle (middle) and both (right), all from NREM stage II of subject 2. Under each sample, a 10–17-Hz band-pass-filtered channel is presented.

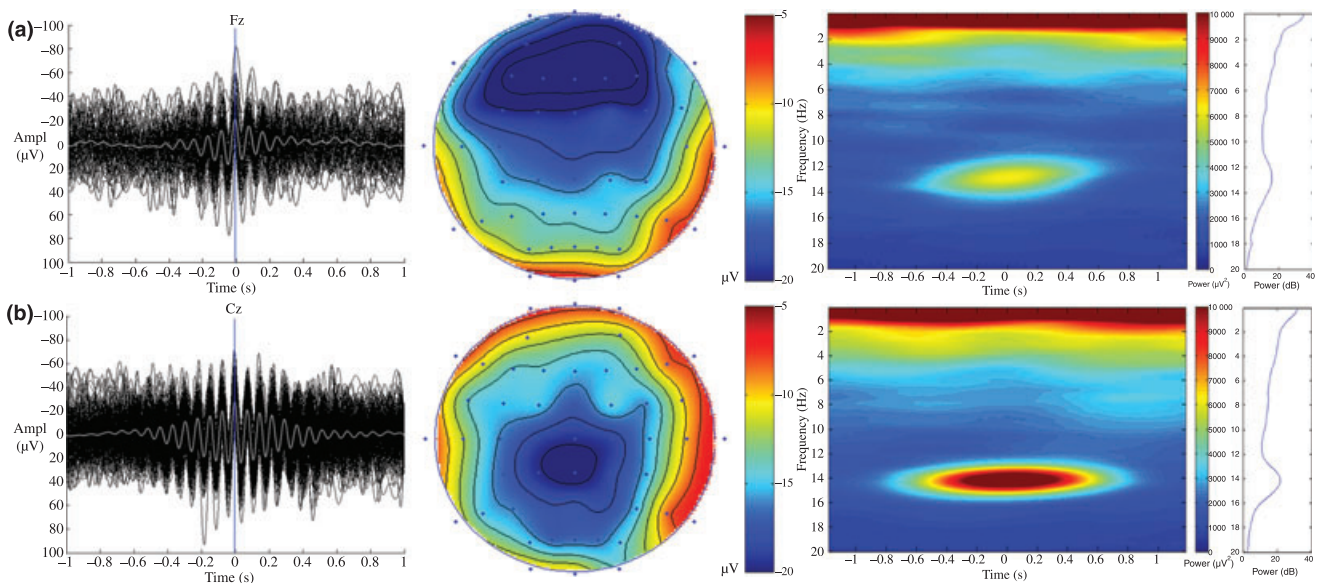


Figure 4. The sleep spindles: on the left, waveform averages (white) and superimposed single traces of 47 slow (a) and 160 fast spindles (b) derived from the Fz and Cz electrode, respectively, taken from the whole-night sleep recording of subject 6. The blue vertical line marks the most prominent negative peak of spindles. Next to them, topographic maps of the most prominent negative peaks derived from the average of slow and fast spindles. On the right, averaged time–frequency analysis of slow and fast spindles derived from the Fz and Cz electrodes, respectively, along with the respective PSD graphs.

characteristics of fast sporadic spindles, that is, they exhibited a waxing–waning shape (see Fig. 5a,b) and had high frequency (14.99 ± 0.90 Hz). The details of sporadic spindles and post-KC spindles frequency comparison are given in Table 2, from which it can be appreciated that the mean frequency of the post-KC spindles was significantly ($P < 0.00001$, paired t -test) higher, in comparison with the fast sporadic spindles of the

same night's sleep, by an average of 0.84 ± 0.12 Hz ($5.93 \pm 0.84\%$).

Sleep spindles are blocked upon KC coincidence

From each subject, during a prime scouting for evidence of KC and sleep spindle interaction, we selected and extracted a total

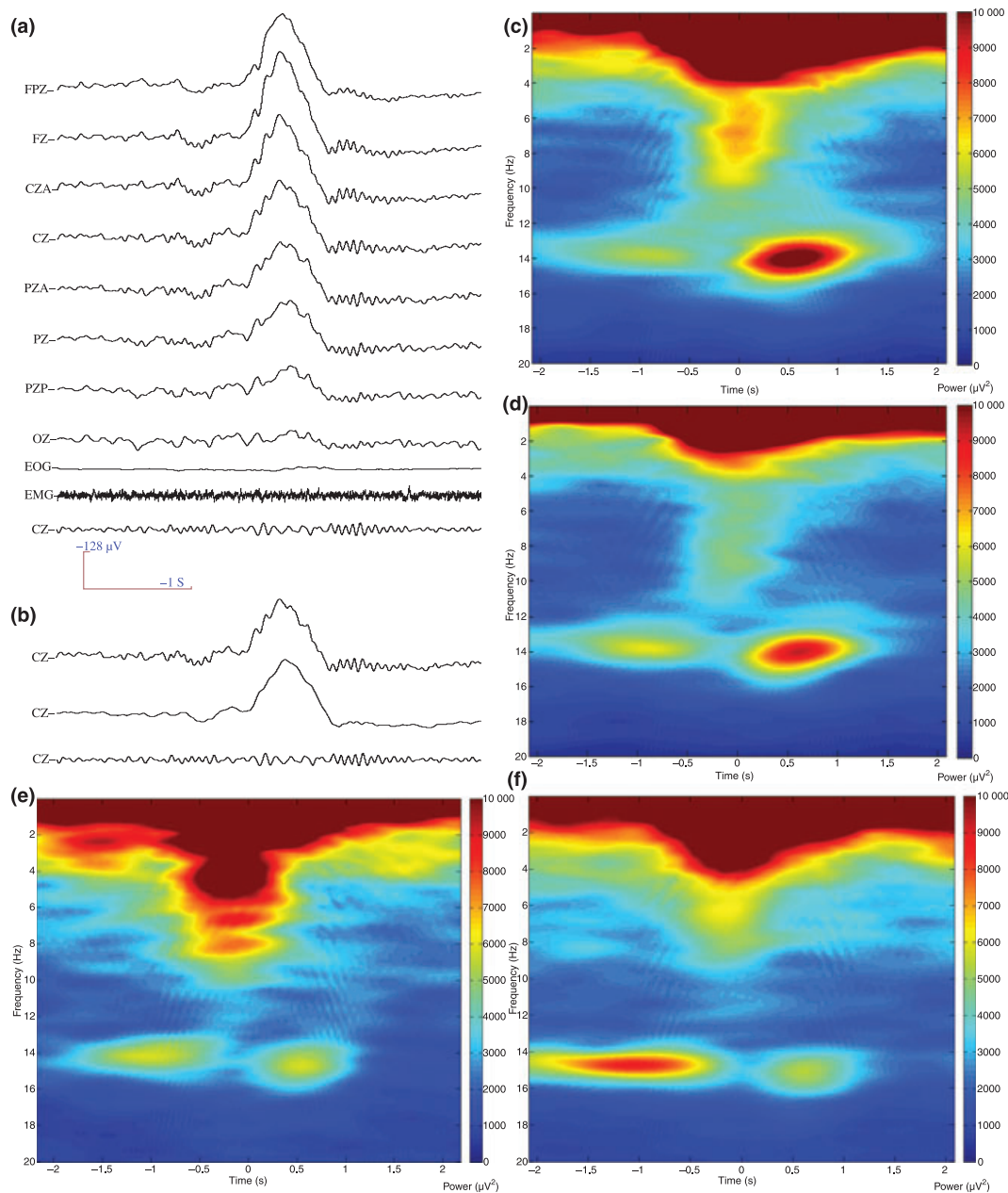


Figure 5. The KC coinciding with spindles: raw EEG from a NREM stage II KC coinciding with a sleep spindle (a). Below, the same sample is shown as raw, 5 Hz low-pass filtered and 6–17 Hz band-pass filtered, from top to bottom, respectively, for the Cz electrode (b). Time–frequency analysis graph of 37 KCs coinciding with spindles (KC_{111}) from subject 1, showing: (a) the blockage of coinciding spindles during the rise of the KC's negative phase; (b) the increase in power of the theta and alpha band (6–10 Hz) around the peak of the negative phase; and (c) the appearance of higher frequency spindles during the fall of the KC's negative and along the positive phase, over electrodes Fz (c) and Cz (d). The average power of post-KC spindles can be higher than pre-KC spindles power (d), can be comparable, as seen from 28 KC_{111} samples of subject 6 (e), and can also be lower, as seen from 54 KC_{111} samples of subject 2 (f), all analyzed over the Cz electrode.

of 403 KCs that occurred while an individual spindle was oscillating. In every case, the development of spindles was interrupted by KCs. The observation of a complete stop in 100% of the cases and the shorter duration on average of these spindles compared with the sporadic ones of the same subject make a coincidental termination of spindles unlikely and allow us to consider it as interruption. Of course, the terms 'interrupted' or 'blocked' are used in their merely descriptive

sense and they do not imply any causal mechanistic relationship.

In the most often appearing case (193/403, 47.89%) these KCs were of the type KC_{111} , that is, KCs that coincide with a spontaneously occurring sleep spindle, present an oscillation during their negative phase and are immediately followed by a new sleep spindle (Fig. 5a). Sample-by sample 6–17-Hz band-pass filtering revealed an interruption of the ongoing sleep

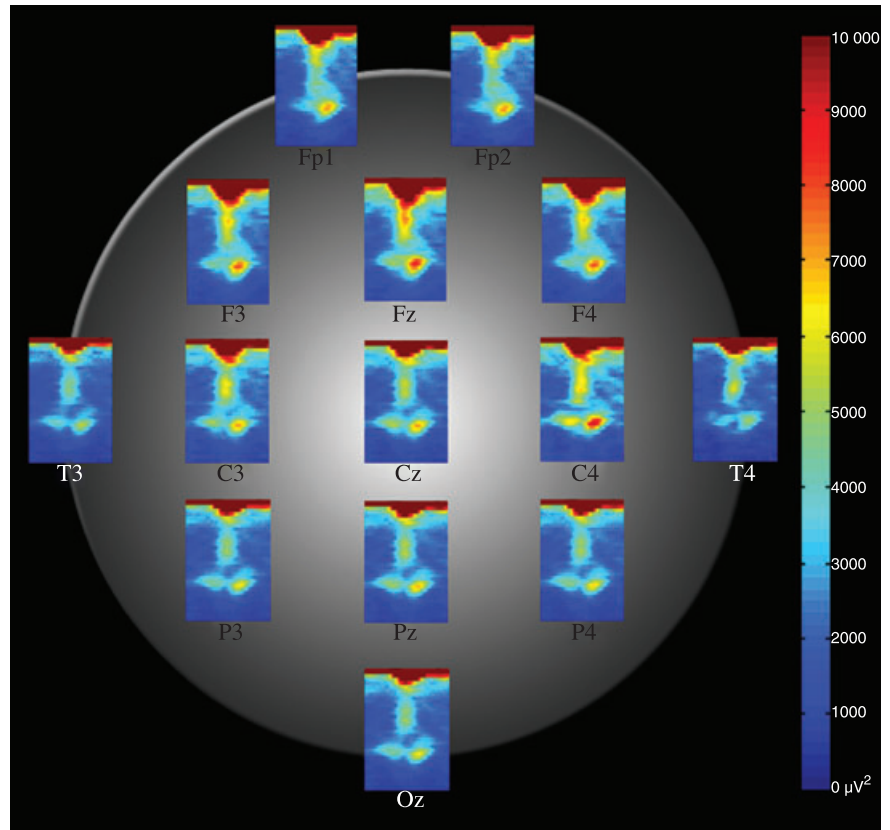


Figure 6. Cortical distribution of the KC versus spindle interaction phenomenon. The interruption of the ongoing spindle upon KC occurrence, the appearance of the intra-KC oscillation, and the generation of a faster post-KC spindle can all be seen in the brain (average time–frequency analysis from 37 KC₁₁₁s of subject 1, as in Fig. 5d). For display density reasons, only the most representative for each lobe electrodes are shown.

Table 4 PSD values of the rhythms in the cases of coincidence of KC with spindles

	Subject 1, PSD (dB)	Subject 2, PSD (dB)	Subject 3, PSD (dB)	Subject 4 (first night), PSD (dB)
Pre-KC spindles	23.13 ± 5.02	26.56 ± 3.88	24.57 ± 3.65	26.32 ± 3.19
KC oscillation	22.57 ± 2.97	25.23 ± 2.98	28.75 ± 2.53	26.97 ± 2.39
Post-KC spindles	24.95 ± 3.00	24.53 ± 3.53	23.91 ± 3.19	26.26 ± 3.12
	Subject 5, PSD (dB)	Subject 6, PSD (dB)	Subject 4 (second night), PSD (dB)	Across-subject means, PSD (dB)
Pre-KC spindles	22.70 ± 3.18	22.62 ± 2.81	25.29 ± 2.78	24.45 ± 1.67
KC oscillation	24.30 ± 2.57	26.18 ± 2.85	27.58 ± 2.38	25.94 ± 2.09
Post-KC spindles	22.27 ± 3.14	23.52 ± 3.06	25.70 ± 2.88	24.44 ± 1.35

By comparing pre-KC with post-KC spindle power, the power relation between them varies from subject to subject. On average the power of the two rhythms remains comparable. Values are means ± SD. The number of samples for each spindle group and subjects are, respectively, those of Table 2.

KC, K-complex; PSD, power spectral density.

spindle during the KC (which we will be referring to as ‘pre-KC spindle’), the appearance of an intra-KC oscillation (8.82 ± 1.20 Hz) in its place and the appearance of a new sleep spindle (Fig. 5b). By ‘intra-KC oscillation’ we want to note that we had no evidence of this oscillation before or after the negative phase of the KC. It seems to characterize most KCs (874/1131, Table 3: KC₀₁₀, KC₀₁₁, KC₁₁₀ and KC₁₁₁), regardless of whether the KCs occur alone (532/708, Table 2: KC₀₁₀ and KC₀₁₁) or during the development of fast spindles (322/403, Table 2: KC₁₁₀ and KC₁₁₁). The probability of KCs being followed by spindles does not seem to depend on whether the KC is crowned by this short rhythmic oscillation

(629/875, 71.96%, Table 2: KC₀₁₁ and KC₁₁₁) or not (186/255, 72.94%, Table 2: KC₀₀₁ and KC₁₀₁).

Sample-by-sample time–frequency analysis covering the time period around the KC negative peak, apart from verifying the spindle interruption and the appearance of a rhythmic oscillation, revealed the generation of a higher frequency spindle by an average of 1.17 ± 0.38 Hz ($8.29 \pm 2.69\%$) after the KC, in comparison to the frequency of the KC-interrupted spindle. Per subject averaging of the KC₁₁₁ time–frequency graphs further confirmed the latter (Fig. 5c,d). The hereby-described prevailing phenomenon of already oscillating spindles being interrupted upon KC occurrence and being replaced

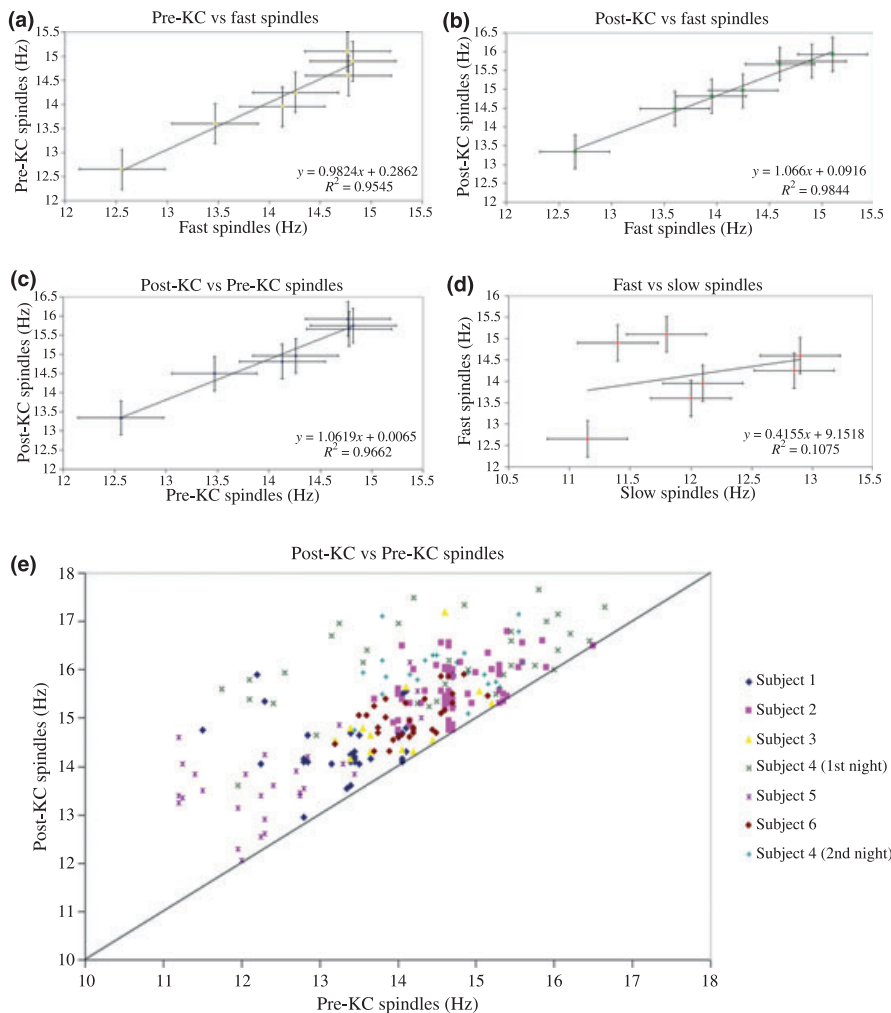


Figure 7. Rhythm relations: pre-KC, fast, and post-KC spindles exhibit a robust relationship (a–c), which does not exist between slow and fast sporadic spindles (d). In each part (a–d), the regression line function appears along with the R^2 value. Note the superior values of the x coefficient and R^2 (both ~ 1) in (a–c) in contrast to the lesser values in (d). (e) The intra-subject relationship between pre-KC and post-KC spindles is shown. Note that the coordinates formed by the frequencies of the two rhythms for each and every EEG trace are always above the midline.

by a short rhythm before a new spindle of higher frequency appeared was observed globally on the scalp (Fig. 6). The frequency of the post-KC spindles was found to be significantly ($P < 0.00001$, paired t -test) higher than the frequency of the fast pre-KC spindles.

The power relation between pre- and post-KC spindles was also investigated. Table 4 shows the mean PSD values for every subject that participated in this study, from which it is clear that the average power relation of the pre- and post-KC spindles varied across subjects. In two of our sleep recordings (subjects 1 and 6), the power of post-KC spindles was higher than the power of pre-KC spindles; in two (subjects 2 and 3) the power of post-KC spindles was lower than the power of pre-KC spindles; and in the rest of our recordings (subjects 4 and 5) the power of the two was kept at the same level (also see Fig. 5, compare d–f).

Relationships between KCs, spindles, and related rhythms

To pursue these findings further, a table of rhythms (TOR) was formed for each subject, denoting the peak frequency of each characteristic brain oscillation and the different types of

spindles were systematically categorized (Table 2). The posterior alpha rhythm, produced under conditions of relaxed awareness, and the two types of sleep spindles are reported for each subject. We added to the TOR the phenomena that are the object of this study, that is, the peak frequencies of the pre-KC spindles, of the rhythmic oscillation appearing during the negative phase of the KC, and of the post-KC spindles, derived from all the accumulated KCs. It is worth noting the relatively consistent frequency means of the above-mentioned rhythms for subject 4 whose sleep was recorded twice. Presenting data from each subject in this TOR reveal that the hereby-described small but robust and consistent effects of KCs can be detected in spite of relatively larger differences of the mean values in each subject (i.e. fast spindles frequency range from 12.65 to 15.10 Hz).

From the TOR, it can also be noted that: (a) the frequency of the posterior alpha rhythm is always lower than that of the slow sporadic spindles; (b) the frequency of the intra-KC oscillation appearing during the negative phase of the KC is always lower than the frequency of both the posterior alpha rhythm and slow spindles; (c) the pre-KC spindles are in congruence with sporadic fast spindles; (d) the frequency of the

post-KC spindles is always higher than the frequency of both fast sporadic and pre-KC spindles. In addition, note the significantly higher proportion of KCs followed by spindles (814/1131, 71.97%) in comparison with KCs preceded by spindles (402/1131, 35.54%).

The relations between the investigated rhythms are schematically depicted in the diagrams of Fig. 7. Fig. 7a–c shows a robust relationship between the frequency of sporadic fast spindles, pre-KC spindles and post-KC spindles, for each of the seven sleep recordings. As Fig. 7b shows, subjects with relatively higher frequency of sporadic spindles also had relatively higher frequency post-KC spindles. More specifically, not only is it shown that the higher the frequency of the sporadic fast spindles (and thereby the frequency of the pre-KC spindles) the higher the frequency of the post-KC spindles, but also that the amount of mean frequency increase is consistent (thus creating the balanced offset of the regression line) irrespective of the mean frequency of the pre-KC spindles. Fig. 7d shows that the latter robustness does not apply amongst slow and fast spindles. In Fig. 7e, the intra-subject pre-KC versus post-KC spindles relationship is shown for all seven sleep recordings. Thus, the ability of spindles oscillating at a higher frequency after the KC is not only shown as a mean difference between evoked and spontaneous fast spindles, but is also observed in each and every one of the 238 cases of individual KCs preceded by spindles and followed by new ones.

As can be noted in Fig. 7a and Table 2, the frequency of fast spindles tends to characterize subjects, that is, it seems to vary more between than within subjects; the span of the mean frequency for each subject (from 12.65 Hz in subject 5–15.10 Hz in subject 4's first night and 14.90 Hz second night) is greater than 2 SD in each subject. For this reason, we compared all parameters of this study in each subject as well as in total, and graphically displayed results for each individual subject. The mean results of comparisons reported have been similarly observed in each and every subject with regards to frequency of spindles (Table 2), but not with regards to their power (Table 4).

To investigate the frequency increase of post-KC spindles in more detail, we separated the pre-KC spindles of every subject into two groups; the first group comprising of pre-KC spindles of frequency that fall below the mean fast spindle frequency (lower frequency group), and the second group of those that exceed the mean (higher frequency group) of each subject. The analysis showed that the post-KC spindles following the lower frequency group exhibited a significantly higher ($P < 0.005$, paired t -test) frequency increase (1.60 ± 0.68 Hz, $11.33 \pm 3.31\%$) than those that followed the higher frequency group (0.74 ± 0.22 Hz, $5.24 \pm 1.55\%$). Thus, we concluded that interruption of lower frequency fast spindles is associated with a higher frequency increase post-KC than the interruption of higher frequency fast spindles. The latter adheres to the existence of a ceiling in spindle frequency increase (and thereby spindle frequency), which is different for each individual subject.

We believed to determine whether the phenomenon of the higher frequency of post-KC spindles had some specific relationship to KC features, and we categorized the selected KCs according to several criteria. First, we clustered KCs according to the $KC_{X-X_0X_+}$ type, as can be seen from the indicative images of Table 3. For each KC type, the mean frequency of the pre-KC spindles, the KC oscillation of the negative phase and the post-KC spindles were once more calculated, as shown in Table 3. By focusing on the four KC types that are related to post-KC spindles (KC_{001} , KC_{011} , KC_{101} , and KC_{111}), one can easily see that the higher post-KC spindle frequency is a common feature. More specifically, post-KC spindle frequency values were higher by an average of 1.21 ± 0.10 Hz ($8.70 \pm 0.71\%$) with respect to those of the respective pre-KC spindles, regardless of the fact that the majority of the accumulated KCs ($KC_{001} + KC_{011} = 577$, 51.01%) were not preceded by spindles but, on the contrary, they were followed by them. When KCs occurred after the appearance of fast spindles (403/1131, 35.63%), spindles invariably (100%) stopped for at least the duration of the rising phase of the KC and were replaced (322/403, 79.9%) by a lower frequency short rhythm of $\sim 8.82 \pm 1.20$ Hz (see raw data of Fig. 5b, and spectral data of Fig. 5c,d). Following this and during the falling phase of their negative phase, a new spindle sequence was evoked in 238/403, 59.05% of the cases. This is a significantly ($P = 0.0009$, paired t -test for the seven sleep recordings) smaller percentage compared with the total cases of KCs that are followed by spindles (815/1131, 72.06%). Apparently, the precedence of spindles decreases the probability of new spindles following the KC (from 72.06% to 59.05%). Hence, there was no case of a spindle running uninterrupted during a KC. Only 21.04% of the total KCs (Table 3, KC_{101} and KC_{111} , total 238/1131) were both preceded and followed by spindles, and in every one of these cases the spindle following was of higher frequency than the one preceding, so it is most likely to be a different event.

Then, aiming to explore a potential dependency of the described effects on the shape or on a particular phase of the KC, we clustered KCs according to their distinguished recorded features, that is, the amplitude of the negative and the positive peak. For each of the abovementioned features, we ranked all accumulated KCs per subject. Then we selected the highest and lowest 25% of the ranked KCs from every subject, waveform-averaged and performed time–frequency analysis on them, as shown in Fig. 8a–d. In all cases, the elevation of post-KC spindle frequency was evident. The mean frequency increase in the 25% of KCs with high negative phase peak for all subjects was 0.95 ± 0.25 Hz, in the 25% of KCs with low negative phase peak was 1.01 ± 0.22 Hz, in the 25% of KCs with high positive peak was 0.93 ± 0.16 Hz, and in the 25% of KCs with low positive phase was 1.00 ± 0.62 Hz. To complement the results, we selected from every subject all KCs whose positive phase was hardly distinguishable and therefore was not marked according to section 'Materials and methods' (Fig. 8e). Even when the positive phase was virtually absent, the post-KC spindles had an average frequency increase of

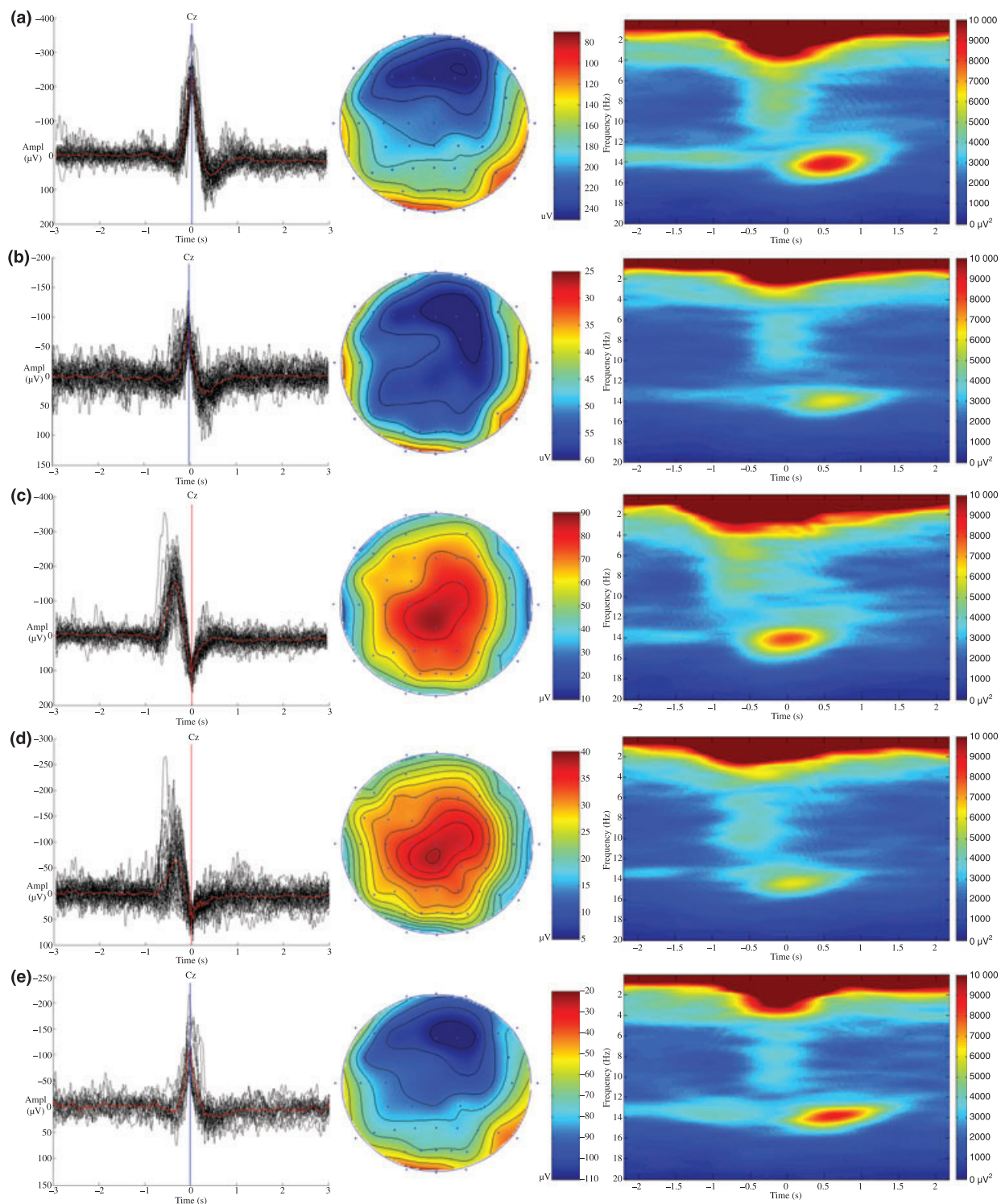


Figure 8. Specificity of post-KC spindle frequency increases. KCs are grouped according to their recorded features and each row displays from left to right superimposed single (black) and averaged (red) waveform (over Cz), topographical and spectral (over Cz) data. (a) KCs of high negative phase peak (the highest 25% of samples, $n = 35$); (b) KCs of low negative phase peak (the lowest 25% of samples, $n = 35$); (c) KCs of high positive phase peak (the highest 25% of samples, $n = 30$); (d) KCs of low positive phase peak (the lowest 25% of samples, $n = 30$); (e) KCs with hardly distinguishable positive phase ($n = 21$). The blue and red vertical lines mark the negative and positive peaks of KCs, respectively. None of these KC features pertains to the generation of higher frequency post-KC spindles (or to the blockage of coinciding pre-KC spindles). All data shown were derived from the clustering of 139 KCs from subject 6.

0.84 ± 0.20 Hz. In addition note that amplitude sorting of both the negative and the positive KC phase (even when the latter is hardly distinguishable) showed that the topographical characteristics did not vary consistently with the KC recorded size (see averages of waveform and topography of Fig. 8).

Finally, we investigated whether the occurrence of post-KC spindles is affected by the occurrence of the distinctive positive phase of the KC. From all subjects, we grouped 811/1131 (71.71%) KCs with prominent positive phase, and 320/1131 (28.29%) with hardly distinguishable positive phase. Of the former group, post-KC spindles occurred at a relatively high proportion of 74.10% (601/811), and in the latter group at an also high and comparable proportion of 66.56% (213/320). It therefore appears that the higher frequency of post-KC spindles is not related to the size or the relative prominence of the KC's positive phase.

DISCUSSION

Detailed analysis of spontaneous singular and generalized KCs occurring during NREM stage II of whole-night undisturbed sleep resulted in three main observations: (a) the sleep spindle is blocked upon accidentally coinciding KC; (b) during the blockage, an intra-KC oscillation appears instead; and (c) the spindles appearing with high probability after the negative peak of the KC – not time-locked to the KC – have a significantly higher frequency than both pre-KC fast spindles as well as sporadic, non-KC-related, fast spindles. The latter increase in spindle frequency was highly correlated to the mean frequency of both the pre-KC spindles and the sporadic fast spindles (Fig. 7), while it seemed to be by a maximum frequency. For every subject all spindle frequencies (sporadic slow and fast, pre- and post-KC spindles) are kept within relatively narrow individual ranges, despite the relatively wider inter-subject variation. Spindle power did not necessarily increase after the KC. Clustering all selected KCs according to the above observations showed that all related combinations (KC_{001} , KC_{011} , KC_{101} , and KC_{111}) exhibited in the immediate post-KC period a similar statistically significant increase in spindle incidence and spectral frequency. The same happened with clusters of KCs with relatively higher or lower amplitude of their negative or positive phases, or even KCs without a positive phase. Finally, the probability of KCs being followed by spindles does not seem to depend on whether the KC is crowned by the short oscillation at ~ 8.8 Hz or not (72% in both). Overall, we found no KC feature that could predict either the spectral frequency increase or the incidence of spindles following the KC better than any others. In all categories, higher frequency spindles occurred after the passing of the KC at a similarly high level of probability. It should be noticed that all conclusions of this study are limited to the prominent type of KCs peaked by unblinded sampling but according to the strict criteria fully described in section 'Materials and methods'; they may not necessarily generalize to all KCs appearing in other sleep stages besides NREM stage II.

In spite of the evidence for independence of spindles from KCs (reviewed in section 'Introduction'), the most frequent clustering of the two graphoelements in the timeframe of the Cyclic Alternating Pattern (Terzano *et al.*, 1985) is impressive. It is often stated that spindles 'ride on KCs' or 'constitute a part of the KC' (Blum and Rutkove, 2007). In addition, the positive phases of KCs are associated to population burst discharges in layer 5 and 6 pyramidal neurons, which project to the thalamus (Amzica and Steriade, 1998). Such a strong corticothalamic input could possibly discharge reticular nucleus (RE) neurons and thereby trigger spindles (Buzsaki, 2006). We have clarified and quantified this tendency to coincide in time, showing that ongoing spindles stop upon KCs for their duration and a new spindle usually appears at the half-second interval following the completion of the negative component of a KC. This study strongly supports the independence of spindles incidence from a preceding KC by means of distinguishing, presenting and analyzing separately all the possible combinations of sequential events/rhythms appearance in association to the KC (KC_{000} – KC_{111} , Table 3), despite the fact that some combinations appear more often than others. If KCs and spindles were not independent phenomena of sleep, at least one of the four combinations (that is, KC_{0X0} , KC_{0X1} , KC_{1X0} and KC_{1X1}) would be obsolete. However, this independence of incidence concerns the generation mechanisms of the KC and the sleep spindle. We have shown in this study that when the two phenomena coincide, there is a clear interaction between the two.

Sleep spindles rhythm is initiated in γ -aminobutyric acid-ergic thalamic RE neurons, which impose onto TC neurons rhythmic inhibitory postsynaptic potentials, thus de-inactivating a low-threshold Ca^{2+} current, which promotes burst firing. This is transferred to the cortex where it induces rhythmic excitatory postsynaptic potentials, the electrical generators of the EEG spindles. Cortical excitation on both RE and TC neurons helps synchronize, spread and maintain the spindle rhythm (Buzsaki, 2006; Steriade and McCarley, 2005). The fact that the ongoing spindling activity is invariably, abruptly and completely blocked upon KC coincidence, the higher spectral frequency and the high incidence of spindles after the negative phase of the KCs are all phenomena that could be understood in the context of the down–up states of the slow frequency (< 1 Hz) cortical oscillation, where the succession of down and up states reflects a hyperpolarizing–depolarizing sequence (Amzica and Steriade, 1998; Cash *et al.*, 2009; Steriade *et al.*, 1993). To the extent that we currently understand the mechanisms of bistability of neocortical networks, it can be surmised that the slow oscillation is an emergent network property of neocortical neurons (Buzsaki, 2006). Scalp-recorded KCs are considered to reflect the neuronal synchrony associated with the down–up depolarization shift (Amzica and Steriade, 1998), and the up state triggers spindles. The fast transition from silence to population activity represents a self-organized criticality, the very nature of which may allow subcortical stimuli (sensory or homeostatic) to interrupt and reverse either the down or up

state. It is therefore conceivable that in our KC_{1XX} types (Table 3) an up state carrying spontaneously occurring spindles was interrupted by an endogenous arousal stimulus, which in turn induced a new down–up shift carrying a KC, and often a new spindle. The higher frequency of the new spindle can then be attributed to a depolarization of TC neurons, which facilitates their rebound firing a few milliseconds earlier than before. In turn, this depolarization of TC neurons could be attributed to either an enhanced corticothalamic input at the beginning of the up state or by the subcortical input that brought about the down–up shift in the first place.

Although both cortical and subcortical effects on the thalamus are possible, we consider the later as better explaining our data, as: (a) RE neurons produce spindles only when a dampening of brainstem activity allows it and that in arousal spindles are blocked when inputs from the brainstem and basal forebrain hyperpolarize and so decouple the synaptic networks of RE (Steriade and McCarley, 2005); (b) KCs may be considered as a complex sleep-protecting reaction to arousing stimuli in the frame of a highly dynamic balance between hypnagogic and arousing tendencies in NREM stage II (Halász, 2005). It is therefore conceivable that a brief arousing stimulus may trigger a KC and at the same time block spindles by a brainstem inhibitory action at the RE level, upon the depolarizing rebound of which a new spindle rhythm of higher frequency is produced. This explanation would be compatible with both the observed higher frequency of spindles occurring immediately after a KC (in each subject faster than the fast and never slow) and the high probability of the post-KC appearing sleep spindles, yet none of the latter correlating with a particular feature of the KC.

Another finding that requires explanation is the appearance during the negative peak of the KC of a short-lasting rhythm of a narrow frequency range (8.88 ± 1.20 Hz). It seems to characterize most KCs, regardless of whether the KCs occur alone (75%) or they occur during the development of fast spindles (80%). Although TC neurons have the ability to produce oscillations in the theta/alpha frequency (Hughes and Crunelli, 2007), these rhythms are not a particular feature of stage II NREM sleep, but rather characterize arousals and partially NREM stage I. While human SWS rhythmic activity in the 12–15-Hz spindle frequency range becomes grouped during the slow oscillations, theta (4–8 Hz) and alpha (8–13 Hz) band activities do not display such dynamics (Möller *et al.*, 2002). The short oscillation we observed during KCs, which appeared to cover a narrow range at the border of these two rhythms, may therefore not relate to either of them. Moreover, we showed (Table 2) that this intra-KC oscillation always had lower frequency than the posterior alpha. Its appearance was not correlated with the appearance of spindles either before or after the KC (Table 3). To our knowledge, this short rhythm has not been observed with other sleep slow waves, like delta. Along with the interaction of the KC with spindles, the revealing of an oscillation riding on the KC negative phase supports the view that the KC is a complex

multifaceted phenomenon, whose secrets are still unveiled seven decades after its first description.

Our data enhance the impression that fast and slow spindles are distinct features of stage II sleep. We confirm (Anderer *et al.*, 2001; Gibbs and Gibbs, 1964; Himanen *et al.*, 2002; Zeitlhofer *et al.*, 1997; Zygierevicz *et al.*, 1999) the frontal predominance and slower frequency compared with the centro-parietal predominance and faster frequency, as well as the relatively higher incidence of the fast spindles (De Gennaro and Ferrara, 2003). In addition, their respective mean spectral frequencies do not appear to co-vary in individual subjects (Fig. 7d). Most crucially, the spindles following KCs were never of the slow type, but actually faster than the fast ones observed in each and every subject.

It is not yet known whether the different characteristics of slow spindles are due to different TC circuits (Anderer *et al.*, 2001) and/or longer hyperpolarization of TC neurons. More frontal slow spindles are found in the first sleep cycle when sleep pressure is assumed to be highest and hyperpolarization of their generators is considered to be deepest (Himanen *et al.*, 2002). Sleep pressure is determined both by homeostatic and circadian factors (Borbély, 1982), and it is difficult to decipher their influence on spindles frequency. Also, our data were pooled from all sleep cycles and we certainly had many very fast spindles in the first cycle of sleep. However, if fast spindles are postulated to occur in instances of relatively lighter sleep compared with the slow ones, the even faster spindles we found to follow KCs may indicate that following the KC there is a short window of time (0.5–2 s) of even lighter sleep than before the KC. This would be in line with the proposed arousing stimulus as a more likely explanation of all the effects we observed.

The frequency variation of sleep spindles provides a handle to the study of TC pacing mechanisms, and our finding of even faster spindles following KC calls for a multidimensional approach that would consider brain location and sleep macrostructure (sleep stages and cycles) as well as microstructure (interaction between concurrent events). Such an approach would help further understand the two roles so far recognized for spindles: the gating of information processing and thus protecting the sleeper from disturbing stimuli (Buzsáki, 2006); and participation in off-line learning (Gais *et al.*, 2002). Spontaneous spindles or TC stimuli in the spindle frequency have been shown to induce sustained depolarization of cortical neurons, enhancement of cortical excitability lasting several minutes and Ca^{2+} entry in the dendrites (Steriade and McCarley, 2005). All these effects are frequency dependent, and learning a visuomotor task has been linked to an increase of fast rather than slow spindles in the cortical areas involved in the learning (Tamaki *et al.*, 2009). Therefore, the observation of even higher frequency spindles could be relevant to brain plasticity and memory consolidation mechanisms. Finally, in the realm of pathophysiology, TC mechanisms elaborating sleep spindles have been implicated in the development of EEG spike and wave discharges underlying absence seizures (evidence reviewed in Kostopoulos, 2000). A gating

function in these discharges has been alternatively ascribed to KCs (Amzica and Steriade, 2002; Halász, 2005). Some information on combining the above hypotheses to explain absence seizures may be given by the observed effects of KCs on spindles.

ACKNOWLEDGEMENTS

The authors acknowledge the contribution of Andreas Koupparis MD in the development of the Matlab-based suite used for sleep data analysis, and Dr Maria L. Stavrinou in signal processing issues.

REFERENCES

- American Academy of Sleep Medicine (AASM). The visual scoring of sleep in adults. *J. Clin. Sleep Med.*, 2007, 3: 121–135.
- American Sleep Disorders Association (ASDA). EEG arousals: scoring rules and examples: A preliminary report from the Sleep Disorder Atlas Task Force of the American Sleep Disorder Association. *Sleep*, 1992, 15: 174–184.
- Amzica, F. and Steriade, M. Cellular substrates and laminar profile of sleep K-complex. *Neuroscience*, 1998, 82: 671–686.
- Amzica, F. and Steriade, M. The functional significance of K-complexes. *Sleep Med. Rev.*, 2002, 6: 139–149.
- Anderer, P., Klossch, G., Gruber, G. *et al.* Low-resolution brain electromagnetic tomography revealed simultaneously active frontal and parietal sleep spindle sources in the human cortex. *Neuroscience*, 2001, 103: 581–592.
- Blum, A. S. and Rutkove, S. B. *The Clinical Neurophysiology Primer*. Humana Press Totowa, New Jersey, 2007.
- Borbély, A. A. A two process model of sleep regulation. *Hum. Neurobiol.*, 1982, 1: 195–204.
- Buzsáki, G. *Rhythms of the Brain*. Oxford University Press, 2006.
- Cash, S. S., Halgren, E., Dehghani, N. *et al.* The human K-complex represents an isolated cortical down-state. *Science*, 2009, 324: 1084–1087.
- Church, M. W., Johnson, L. C. and Seales, D. M. Evoked K-complexes and cardiovascular responses to spindle-synchronous and spindle-asynchronous stimulus clicks during NREM sleep. *Electroencephalogr. Clin. Neurophysiol.*, 1978, 45: 443–453.
- Colrain, I. M. The K-complex: a 7-decade history. *Sleep*, 2005, 28: 255–273.
- Crowley, K., Trinder, J., Colrain, I. and Evoked K-complex generation: the impact of sleep spindles, age. *Clin. Neurophysiol.*, 2004, 115: 471–476.
- Curcio, G., Ferrara, M., Pellicciari, M. C., Cristiani, R. and DeGennaro, L. Effect of total sleep deprivation on the landmarks of stage 2 sleep. *Clin. Neurophysiol.*, 2003, 114: 2279–2285.
- De Gennaro, L. and Ferrara, M. Sleep spindles: an overview. *Sleep Med. Rev.*, 2003, 7: 423–440.
- De Gennaro, L., Ferrara, M. and Bertini, M. The spontaneous K-complex during stage 2 sleep: is it the “forerunner” of delta waves? *Neurosci. Lett.*, 2000, 291: 41–43.
- DGSM German Sleep Society Task Force. A review of sleep EEG patterns. Part I: A compilation of amended rules for their visual recognition according to Rechtschaffen and Kales. *Somnologie*, 2006, 10: 159–175.
- Ehrhart, J., Ehrhart, M., Muzet, A., Schieber, J. P. and Naitoh, P. K-complexes and sleep spindles before transient activation during sleep. *Sleep*, 1981, 4: 400–407.
- Gaillard, J. M. and Tissot, R. EEG sleep studies of insomniacs under flunitrazepam treatment. *Int. Pharmacopsychiatry*, 1975, 10: 199–207.
- Gais, S., Molle, M., Hels, K. and Born, J. Learning-dependent increase in sleep spindle density. *J. Neurosci.*, 2002, 22: 6830–6834.
- Gibbs, F. A. and Gibbs, E. L. In: A. Reading (Ed.) *Atlas of Electroencephalography*, Vol. 1. Addison-Wesley, Reading, MA, USA, 1964: 90–96.
- Halász, P. Arousals without awakening – dynamic aspect of sleep. *Physiol. Behav.*, 1993, 54: 795–802.
- Halász, P. K-complex, a reactive graphoelement of NREM sleep: an old chap in a new garment. *Sleep Med. Rev.*, 2005, 9: 391–412.
- Himanen, S.-L., Virkkala, J., Huhtala, H. and Hasan, J. Spindle frequencies in sleep EEG show U-shape within first four NREM sleep episodes. *J. Sleep Res.*, 2002, 11: 35–42.
- Hornyak, M., Cejnar, M., Elam, M., Matousek, M. and Wallin, B. G. Sympathetic muscle nerve activity during sleep in man. *Brain*, 1991, 114: 1281–1295.
- Hughes, S. W. and Crunelli, V. Just a phase they’re going through: the complex interaction of intrinsic high-threshold bursting and gap junctions in the generation of thalamic alpha and theta rhythms. *Int. J. Psychophysiol.*, 2007, 64: 3–17.
- Johnson, L. C., Hanson, K. and Bickford, R. G. Effect of flurazepam on sleep spindles and K-complexes. *Electroenceph. Clin. Neurophysiol.*, 1976, 40: 67–77.
- Kostopoulos, G. K. Spike-and-wave discharges of absence seizures as a transformation of sleep spindles: the continuing development of a hypothesis. *Clin. Neurophysiol.*, 2000, 111(Suppl. 2): S27–38.
- Kubicki, S., Haag-Wusthof, C., Rohmel, J., Hermann, W. M. and Scheuler, W. Effect of lormetazepam, triazolam and flunitrazepam on rapid eye movements, K-complexes and sleep spindles in normal probands [in German]. *EEG EMG Z. Elektroenzephalogr. Elektromyogr. Verwandte Geb.*, 1987, 18: 61–67.
- Loomis, A. L., Harvey, E. N. and Hobart, G. A. Electrical potentials of the human brain. *J. Exp. Psychol.*, 1936, 19: 249–279.
- Loomis, A. L., Harvey, E. N. and Hobart, G. A. Distribution of disturbance patterns in the human electroencephalogram, with special reference to sleep. *J. Neurophysiol.*, 1938, 1: 413–430.
- Mölle, M., Marshall, L., Gais, S. and Born, J. Grouping of spindle activity during slow oscillations in human non-rapid eye movement sleep. *J. Neurosci.*, 2002, 22: 10941–10947.
- Naitoh, P., Antony-Baas, V., Muzet, A. and Ehrhart, J. Dynamic relation of sleep spindles and K-complexes to spontaneous phasic arousal in sleeping human subjects. *Sleep*, 1982, 5: 58–72.
- Okada, H., Iwase, S., Mano, T., Sugiyama, Y. and Watanabe, T. Changes in muscle sympathetic nerve activity during sleep in humans. *Neurology*, 1991, 41: 1961–1966.
- Rechtschaffen, A. and Kales, A. (Eds) *A Manual of Standardized Terminology, Techniques and Scoring System for Sleep Stages of Human Subjects*. BI/BR, Los Angeles, CA, 1968.
- Roth, M., Shaw, J. and Green, J. The form, voltage distribution and physiological significance of the K-complex. *Electroenceph. Clin. Neurophysiol.*, 1956, 8: 385–402.
- Sandwell, D. Biharmonic spline interpolation of GEOS-3 and SEAS-TAT altimeter data. *Geophys. Res. Lett.*, 1987, 14: 139–142.
- Schabus, M., Dang-Vu, T. T., Albouy, G. *et al.* Hemodynamic cerebral correlates of sleep spindles during human non-rapid eye movement sleep. *Proc. Natl Acad. Sci. USA*, 2007, 104: 13164–13169.
- Steriade, M. and McCarley, R. W. *Brain Control of Wakefulness and Sleep*. Springer, New York, 2005.
- Steriade, M., Nunez, A. and Amzica, F. A novel slow (<1 Hz) oscillation of neocortical neurons *in vivo*: depolarizing and hyperpolarizing components. *J. Neurosci.*, 1993, 13: 3252–3265.
- Takeuchi, S., Iwase, S., Mano, T., Okada, H., Sugiyama, Y. and Watanabe, T. Sleep-related changes in human muscle and skin sympathetic nerve activities. *J. Auton. Nerv. Syst.*, 1994, 47: 121–129.

- Tamaki, M., Matsuoka, T., Nittono, H. and Hori, T. Activation of fast sleep spindles at the premotor cortex and parietal areas contributes to motor learning: a study using sLORETA. *Clin. Neurophysiol.*, 2009, 120: 878–886.
- Tank, J., Dietrich, A., Hale, N. *et al.* Relationship between blood pressure, sleep K-complexes, and muscle sympathetic nerve activity in humans. *Am. J. Physiol. Regul. Integr. Comp. Physiol.*, 2003, 285: R208–214.
- Terzano, M. G., Mancina, D., Salati, M. R., Costani, G., Decembrino, A. and Parrino, L. The cyclic alternating pattern as a physiologic component of normal NREM sleep. *Sleep*, 1985, 8: 137–145.
- Urakami, Y. Relationships between sleep spindles and activities of cerebral cortex as determined by simultaneous EEG and MEG recording. *J. Clin. Neurophysiol.*, 2008, 25: 13–24.
- Yamadori, A. Role of spindles in the onset of sleep. *J. Med. Sci.*, 1971, 17: 97–111.
- Zeitlhofer, J., Gruber, G., Anderer, P., Asenbaum, S., Schimicek, P. and Saletu, B. Topographic distribution of sleep spindles in young healthy subjects. *J. Sleep Res.*, 1997, 6: 149–155.
- Zygierewicz, J., Blinowska, K. J., Durka, P. J., Szelenberger, W., Niemcewicz, S. and Androsiuk, W. High resolution study of sleep spindles. *Clin. Neurophysiol.*, 1999, 110: 2136–2147.